https://doi.org/10.33805/2690-2575-110
Volume 2 Issue 1 | PDF 110 | Pages 5

EDELWEISS PUBLICATIONS
OPEN ACCESS

Nanomaterial Chemistry and Technology

Research Article ISSN: 2690-2575

Ionic Liquids/SiO_2 Supporting Pd Nanoparticles: Efficient Catalysts in Hydrogenation Reaction

Taís Hartz[1], Daiane Fischer[1], Karina de Fraga[1] and Carla Scheeren[1*]

Affiliation: [1]Laboratory of Catalysis, School of Chemistry and Food, Federal University of Rio Grande - FURG, Rua Barão do Caí, Brazil

[*]**Corresponding author:** Carla Scheerena Laboratory of Catalysis, School of Chemistry and Food, Federal University of Rio Grande - FURG, Rua Barão do Caí, 125, CEP 95500-000, Santo Antônio da Patrulha, RS, Brazil. Email: carlascheeren@gmail.com

Citation: Hartz T, Fischer D, de Fraga K and Scheeren C. Ionic liquids/SiO_2 supporting Pd nanoparticles: efficient catalysts in hydrogenation reaction (2021) Nanomaterial Chem Technol 2: 8-12.

Received: Aug 26, 2021
Accepted: Sep 21, 2021
Published: Oct 11, 2021

Abstract

Palladium nanoparticles (ca. 4.8 nm) were synthesized in presence of 1-n-butyl-3-methylimidazolium tetraflouroborate (BMI.BF_4) and 1-n-butyl-3-methylimidazolium hexafluorophosphate (BMI.PF_6) and PMI.Si.$(OMe)_3$.Cl functionalized ionic liquids using the sol-gel method. The characteristics of the sol-gel method, ionic liquid on the palladium content was studied, as well as the silica morphology and texture of the support and the hydrogenation activity. The palladium content in the resulting xerogels (ca. 0.22 wt% Pd/SiO_2) was shown to be independent of the sol-gel process. The xerogels synthesized in acidic conditions formed materials with larger pore diameters, which in turn might be responsible for the higher catalytic activity in hydrogenation of the alkenes and arenes obtained with the heterogeneous catalyst (Pd/ILs/SiO_2).

Keywords: Nanoparticles, Material, Chromatography.

Abbreviations: IIL-Imidazolium Ionic Liquids, MNP- The Metal Nanoparticles, ED- Electron Diffraction, TEOS- Tetraethoxy Orthosilicate, XRD- X-Ray Diffraction, RBS- Rutherford Backscattering Spectrometry, TEM- Transmission Electron Microscopy.

Introduction

Palladium catalysts supported are used in various processes including amination, Heck and Suzuki coupling, hydrogenation, hydrogen production and dehydrogenation reactions [1-15]. The Pd/SiO_2 is a classical model of Pd catalysts with SiO_2 as the "inert" oxide support [16]. SiO_2 resists to reduction and has low surface acidity, making it relatively inert compared to other oxide supports, such as TiO_2 and Al_2O_3 [17]. These characteristics make Pd/SiO_2 an ideal starting point for study of the catalytic role of Pd [18,19]. It is well known that several steps in the catalyst preparation process strongly influence particle size, including the support composition, metal salt, precursor deposition method, metal loading, pH, drying conditions, calcinations temperature, and reduction temperature, among others [20,21].

The combination of an ionic liquid with a solid support material is emerging as a new alternative for the immobilization of transition metal catalyst precursors [22,23]. Imidazolium Ionic Liquids (ILs) possess pre-organized structures mainly through hydrogen bonds which induce structural directionality [24]. These IL structures can adapt or be adaptable to many species, as they provide hydrophobic or hydrophilic regions, and a high directional polarizability [25,26].

This structural organization of ILs can be used as "entropic drivers" for spontaneous, well-defined and extended ordering of nanoscale structures. Indeed, the unique combination of adaptability towards Other molecules and phases associated to the strong hydrogen-bond driven structure makes ionic liquids potential key tools in the Preparation of a new generation of chemical nanostructures such as template porous silica prepared in a sol-gel process [27-30].

The Metal Nanoparticles (MNPs) with small diameter and narrow size distribution can be prepared by simple H_2 reduction of metal compounds or decomposition of organometallic species dissolved in ILs [31-32]. In several cases the MNPs are not stable and tend to aggregate [33]. Alternatively, these nanoparticles can be used in conjunction with other stabilizers or be easily transferred to other organic and inorganic supports to generate more stable and active catalysts [34-37] The metal nanoparticles/ionic liquid/stabilizer combination usually exhibits an excellent synergistic effect that enhances activity of the catalyst. So could be prepared more efficient and stable catalytic systems using the generation of metal nanoparticles associated with silica using ILs as templates for both catalytic partners i.e. the metal nanoparticles and the silica support [38-42].

We present herein our results, which show that palladium nanoparticles synthesized in BMI.BF_4, BMI.PF_6 and PMI.Si.$(OMe)_3$.Cl ionic liquids can be applied for the generation of the heterogeneous catalyst (Pd/ILs/SiO_2) via sol-gel processes. The heterogeneous catalyst formed (Pd/ILs/SiO_2) was applied in hydrogenation reactions studies.

Experimental

General

All experiments were performed in air, except for the synthesis of the Pd NPs. The Pd NPs and the halide-free BMI.PF_6, BMI.BF_4 and PMI.Si.$(OMe)_3$.Cl ionic liquids were prepared according to literature procedure [33,43]. Solvents, alkenes, and arenes were dried with the appropriate drying agents and distilled under argon prior to use. All other chemicals were purchased from commercial sources and used without further purification. Gas chromatography analysis was

performed with a Hewlett-Packard-5890 gas chromatograph with an FID detector and a 30 m capillary column with a dimethylpolysiloxane stationary phase. The nanoparticles formation and hydrogenation reactions were carried out in a modified Fischer–Porter bottle immersed in a silicone oil bath and connected to a hydrogen tank. The temperature was maintained at 75 °C by a hot-stirring plate.

Synthesis of Palladium Nanoparticles (Pd NPs) supported in silica and ILs: Silica supporting Pd NPs/ILs/SiO_2 were prepared by the sol-gel method under acidic conditions. Typical procedure for acid catalysis: 10 mL of tetraethoxy orthosilicate (9.34 g, 45 mmol) was introduced in a Becker under vigorous stirring at 60 °C. The Pd NPs/ILs (10 mg, 0,05 mmol) dispersed in BMI.PF_6, BMI.BF_4 and PMI.Si.$(OMe)_3$.Cl ionic liquids (1 mL, 5.1 mmol) and ethanol (5 mL). This solution was submitted to stirring and sonication for 2 min and then added to the solution containing TEOS. Consecutively, an acid solution (HF) was added as acid catalyst.

The temperature was kept at 60 °C for 18 h. The resulting material was washed several times with acetone and dried under vacuum. Typical procedure for base catalysis: 10 mL of TEOS (9.34 g, 45 mmol) was added to ethanol (5 mL), containing the ionic liquids (1 mL, 5.1 mmol) and previously isolated Pd NPs (10 mg, 0.05 mmol). Then ethanol (95 mL) and ammonium hydroxide (20 mL) were added. The mixture was kept under stirring for 3 h at room temperature and left to stand for a further 18 h. The resulting xerogel was filtered and washed with acetone and dried under vacuum for 1 h.

X-Ray Diffraction (XRD)

The phase structures were characterized by of XRD Pd NPs. For XRD analysis, the nanoparticles were isolated as a fine powder and placed on the specimen holder. The XRD experiments were performed in a SIEMENS D500 diffractometer equipped with a curved graphite crystal using radiation Cu K ∞ (λ = 1.5406 Å). The diffraction data were collected at room temperature in Bragg-Brentano geometry Θ-2 Θ. The equipment was operated at 40 kV and 20 mA with a scan range between 20° and 90°. The diffractograms were obtained with a constant step Δ2Θ = 0.05. The indexation of Bragg reflections was obtained by fitting a pseudo-Voigt profile using the code FULPROFF code.37 Nanoparticles Pd/ILs/SiO2 were analyzed on a glass substrate.

Elemental analysis (CHN)

The organic phases present in the xerogels were analyzed using CHN elemental Perkin Elmer elemental CHNS/O analyzer, model 400. Triplicate analysis of the samples, previously heated at 100 °C under vacuum for 1 h, was carried out.

Rutherford Backscattering Spectrometry (RBS)

Palladium loadings in catalysts were determined by RBS using He+ beams of 2.0 MeV incidents on homogeneous tablets of the compressed (12MPa) catalyst powder. The method is based on the determination of the number and energy of the detected particles, which are elastically scattered in the Coulombic field of the atomic nuclei in the target. In this study, the Pd/Si atomic ratio was determined by the heights of the signals corresponding to each of the elements in the spectra and converted to wt% Pd/ILs/SiO_2. For an introduction to the method and applications of this technique, the reader is referred elsewhere.

Nitrogen adsorption-desorption isotherms

The adsorption–desorption isotherms of previous degassed solids (150 °C) were determined at liquid nitrogen boiling point in a volumetric apparatus, using nitrogen as probe. The specific surface areas of xerogels were determined from the t-plot analysis and pore size distribution was obtained using the BJH method. A homemade equipment with a vacuum line system employing a turbo-molecular Edwards vacuum pump was used. The pressure measurements were made using a capillary Hg barometer and a Pirani gauge.

Scanning Electron Microscopy (SEM) and Electron Dispersive Spectroscopy (EDS) elemental analysis

The materials were analyzed by SEM using a JEOL model JSM 5800 with 20 kV and 1000 magnification. The same instrument with was used for the EDS with a Noran detector (20 kV and acquisition time of 100 s and 1000 magnification).

Transmission Electron Microscopy (TEM) analysis

The morphologies and the Electron Diffraction (ED) patterns of the obtained particles were determined on a JEOL JEM-2010 equipped with an EDS system and a JEOL JEM-120 EXII electron microscope, operating at accelerating voltages of 200 and 120 kV, respectively. The TEM samples were prepared by deposition of the Pd NPs or Pd/ILs/SiO_2 isopropanol dispersions on a carbon-coated copper grid at room temperature. The histograms of the nanoparticle size distributions were obtained from the measurement of around 300 diameters and reproduced in different regions of the Cu grid assuming spherical shapes.

Catalytic Hydrogenations

The catalysts (150 mg) were placed in a Fischer–Porter bottle and the alkene or arene (12.5 mmol) was added. The reactor was placed in an oil bath at 75 °C and hydrogen was admitted to the system at constant pressure (4 atm) under stirring until the consumption of hydrogen stopped. The organic products were recovered by decantation and analyzed by GC.

Results and Discussion

The sol-gel process involves a chemical approach for the synthesis of stable oxide materials, this process allows us to obtain solid products by creating an oxide network via progressive polycondensation reactions in a liquid medium [41]. The steps involved consist of hydrolysis and condensation. The reactions are affected by the nature of the catalyst. Therefore, in the present study, two main routes were evaluated: (i) an acid-catalyzed one using either HF, or (ii) a base-catalyzed approach, using NH_4OH as catalyst. In both routes, the hydrolysis and condensation of Tetraethoxy Orthosilicate (TEOS) were performed in the presence of Pd NPs, which were prepared by hydrogen reduction (4 atm) of $Pd_2(dba)_3$ dissolved in the ionic liquids at 75 °C [27]. These nanoparticles obtained presented 4.8 nm of diameter.

Figure 1 shows the XRD pattern of Pd NPs and encapsulated in silica matrix showing the diffraction planes of silica and Platinum (Pd/ILs/SiO_2). This material was obtained by sol-gel synthesis under acidic conditions using the liquids amount of Pd (0) < 0.2% compared to silica. These Pd nanoparticles were first isolated from the IL to be characterized by XRD (Figure 1A). Through the analysis of X-Ray Diffraction (XRD), is possible identified crystalline palladium in the isolated powder. The characteristics diffraction lines (111, 220, 200, 311) of metallic Pd can be observed in the diffraction pattern (Figure 1A). The Pd NPs obtained presented 4.8±0.4 nm with a narrow range of diameter distribution. The Figure 1B show the Pd/ILs/SiO_2 XRD, diffraction lines (111 and 220) were detected in the sample.

TEM analysis of the synthesized Pd NPs show that the particles display a spherical shape. The mean diameter observed was 4.8±0.4 nm Pd NPs estimated from ensembles of 300 particles found in an arbitrary chosen area of the enlarged micrographs. The evaluation of their characteristic diameter results in a monomodal particle size distribution (**Figure 2A**). Figure 2B show the obtained particle size distributions that can be reasonably well fitted by a Gaussian curve.

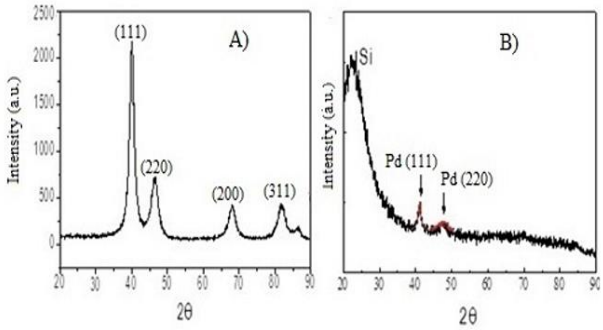

Figure 1: XRD analysis of: A) Pd NPs (4.8 nm) and B) Pd NPs/IL/SiO_2.

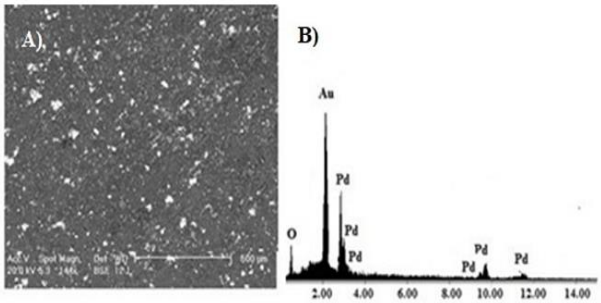

Figure 2: SEM micrographs obtained of: A) Pd NPs/ILs/SiO2 and B) EDX corresponding.

Table 1 present the elemental analysis of the resulting silica. Carbon and nitrogen content was taken as a sign for the presence of ionic liquids once encapsulated within the silica network. Based on the results shown in Table 1, higher ionic liquids contents were incorporated with the acid catalysts. It is worth noting that in the case of acidic conditions, hydrolysis is faster than condensation.

Entry	Sample	M ($\mu g\ g^{-1}$)	M % (m/m)
1	Pd /SiO_2/NH_4OH	2.7	1.9
2	Pd /SiO_2/HF	4.4	1.4
3	Pd /SiO_2/NH_4OHBMI.PF_6	5.6	1.8
4	Pd /SiO_2/HF/BMI.Cl	8.8	2.3
5	Pd /SiO_2/NH_4OH/BMI.Cl	12	3.2
6	Pd/SiO_2/HF/MIPSi$(OMe)_3$.Cl	15	4.1
7	Pd/SiO_2/NH_4OH/MIPSi$(OMe)_3$.Cl	11	4.6
8	Pd/SiO_2/HF/MIPSi$(OMe)_3$.NTf_2	12	5.1
9	Pd /SiO_2/NH_4OH/MIPSi$(OMe)_3$.NTf_2	12	4.6
[a] Determined by RBS.			

Table 1: Elemental analysis of samples Pd/ILs/SiO_2.

The rate of condensation slows down with increasing number of siloxane linkages around a central silicon atom. This leads to formation weakly branched polymeric networks. The condensation, in case of basic conditions, is accelerated relative to hydrolysis. The rate of condensation increases with increasing number of siloxane bridges, result in highly branched networks are formed [42,43]. In the present case, based on the carbon and nitrogen contents, it seems that the resulting weakly branched structure generated in the presence of acid catalyst (either HF) guarantees the constraint of the ionic liquids.

Rutherford Backscattering Spectrometry (RBS) was used in the determination of the metal contents. The Table 1 show that the immobilized Pd content is roughly the same for silica prepared by both routes, corresponding to ca. 65-75% of the initial Pd content employed in the synthesis. The metal distribution in the support was determined by SEM-EDX analyses. Mapping showed a homogeneous Palladium distribution in the silica grains, independently of the preparative route. The Figure 2 shows SEM micrograph of Pd/ILs/SiO_2 synthesized using acid conditions by sol-gel method. The micrograph show lighter regions, indicating the presence of platinum metal nanoparticles on the silica matrix (gray regions). The elemental composition of the region focused on the micrograph confirms this structure. Samples Pd/ILs/SiO_2 were analyzed by the scanning point and area exposed to the electron beam.

All selected areas showed the presence of palladium in the silica matrix. In the micrograph, the metal is identified by the bright regions in contrast to the array of silicon that has the dark background. **Figure 3** illustrates the micrography of Pd/ILs/SiO_2 prepared by both routes, acid and basic. According to Figure 3, particle morphologies are in accordance to that usually observed for pure silica synthesized by these routes. In the case of acid-catalyzed conditions, a less organized, plate-like structure was observed, while in the case of basic conditions, spherical particles were obtained. It is worth noting that smaller particles were produced in the latter case.

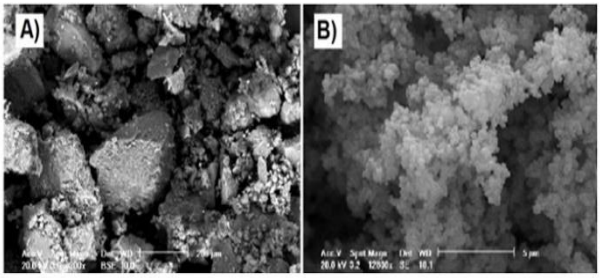

Figure 3: Micrographs obtained by SEM of the resulting xerogels: (A) Pd/ILs/ SiO_2/HF/ (acid) and B) Pd/ILs/ SiO_2/NH_4OH (basic).

Transmission Electron Microscopy (TEM) was also employed for the characterization of the supported catalyst. **Figure 4** shows the micrograph of the Pd/ILs/SiO_2, the mean size of which was shown to be ca. 4.8 nm. It is very likely that the presence of ionic liquids affords stability, avoiding sintering of the metallic particles.

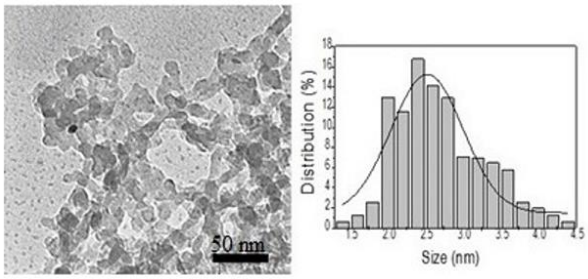

Figure 4: Micrographs obtained by TEM of Pd/ILs/SiO2/HF and histogram of diameter distribution.

The textural properties were further characterized by nitrogen adsorption. Specific area was calculated by the BET method, while pore diameter, by the BJH one (**Table 2**). According to Table 2, silica prepared in the absence of palladium present higher specific area (ca. 100 $m^2\ g^{-1}$). The introduction of nanoparticles during the synthesis, independently of the synthetic route, led to a reduction in the specific area. The pore diameter was demonstrated to be smaller for the materials was used NH_4OH as catalyst. The pore volume was shown to be independent of the presence of Pd in acidic or basic conditions. The supported catalysts were evaluated in hydrogenation reactions.

Table 3 presents data regarding 1-decene, cyclohexene and benzene hydrogenation reactions. For comparative purposes we also included the data concerning the catalytic activity of isolated Pd NPs [27].

Entry	Sample	*SB* ET/ m^2 g^{-1}	*Vp*/cm ^{3} g^{-1}	*dp*/nm
1	SiO_2/HF	168	0.15	1.9
2	SiO_2/HF/BMI.BF_4	122	0.2	8.2
3	SiO_2/HF/BMI.PF_6	36	0.021	1.9
4	SiO_2/NH_4OH/BMI.BF_4	120	0.2	4.3
5	SiO_2/HF/BMI.BF_4	108	0.07	4.2
6	SiO_2/ NH_4OH/BMI.BF_4	5.8	0.008	19
7	SiO_2/ HF/MIPSi(OMe)$_3$.Cl	68	0.02	3.8
8	SiO_2/ NH_4OH/MIPSi(OMe)$_3$.Cl	188	0.27	2.7
9	SiO_2/ HF/MIPSi(OMe)$_3$.N(Tf)$_2$	84	0.28	5.4
10	SiO_2/ NH_4OH/MIPSi(OMe)$_3$.N(Tf)$_2$	221	0.24	2.6
11	SiO_2/HF/MIPSi(OMe)$_3$.PF_6	232	0.22	2.4
12	SiO_2/ NH_4OH/MIPSi(OMe)$_3$.PF_6	242	0.3	2.8
[a]S_{BET}= specific area determined by BET method. *Vp*= pore volume, *dp*= pore diameter.				

Table 2: Surface area, pore volume and average pore diameter of SiO_2/ILs supporting Pd NPsa.

Ent.	Catalyst	Ionic Liquid	Substrate	Time (h)	Conv. %	TOF (min^{-1})
1	[a]HF	BMI.BF_4	1-Decene	0.4	99	1547
2	[a]HF	BMI.BF_4	Cyclohexene	0.8	99	773
3	[a]HF	BMI.BF_4	Benzene	18	96	33
4	[a]NH_4OH	BMI.BF_4	1-Decene	2.5	99	247
5	[a]NH_4OH	BMI.BF_4	Cyclohexene	6	97	101
6	[a]NH_4OH	BMI.BF_4	Benzene	-	-	-
7	[b]HF	BMI.PF_6	1-Decene	0.6	99	1041
8	[b]HF	BMI.PF_6	Cyclohexene	3	93	194
9	[b]HF	BMI.BF_4	1-Decene	0,3	99	2062
10	[c]Pd/SiO_2	BMI.BF_4	1-Decene	0.6	99	1031
11	[c]Pd/SiO_2	BMI.BF_4	Cyclohexene	1	99	618
12	[c]Pd/SiO_2	BMI.BF_4	Benzene	9	96	68.7
13	HF	MIPSi(OMe)$_3$.N(Tf)$_2$	1-Decene	0.15	99	4166
14	NH_4OH	MIPSi(OMe)$_3$.N(Tf)$_2$	Cyclohexene	1.2	99	520
15	HF	MIPSi(OMe)$_3$.PF_6	1-Decene	0.6	99	1041
16	NH_4OH	MIPSi(OMe)$_3$.PF_6	1-Decene	0.8	98	781
17	HF	MIPSi(OMe)$_3$.Cl	1-Decene	0.5	99	1237
18	NH_4OH	MIPSi(OMe)$_3$.Cl	1-Decene	1.1	99	562
19	HF	MIPSi(OMe)$_3$.PF_6	1-Decene	0.7	98	892
20	[d]$Pd_2(dba)_3$	-	1-Decene	0.6	100	416
21	[d]Pd NPs	-	1-Decene	0.9	100	277
22	[d]Pd NPs	-	Cyclohexene	1.6	100	156
23	[d]Pd NPs	-	Benzene	10	100	25

A) Reactions conditions: sol-gel method, constant hydrogen pressure (4 atm), 75 °C ratio [alkene/Arene]/[Pd/SiO2] = 1250/1, added Pd/SiO2 (150 mg, 0.010 mol Pd NPs followed by 12.5 mmol of alkenes or arenes. **B)** grafting method constant hydrogen pressure (4 atm), 75 °C ratio [alkene/Arene]/Pd/SiO2] = 625/1, SiO2 added (150 mg, 0.025 mmol Pd followed by 12.5 mmol the arenes used**. C)** Pd nanoparticles (5 mg. Relation [Arene]/[Pd]] = 250/1, added Pd (5 mg. **D)** Pd NPs [alkene/arene]/[metal(0)]= 250/1) followed by 12.5 mmol of alkenes or arenes.

Table 3: Hydrogenation of alkenes by encapsulated Pd/ILs/SiO2a and Pd NPsb.

Table 3 shows the results obtained in the hydrogenation reactions using the system Pd/SiO_2. Is possible to observe that all the supported systems were more active than those constituted of isolated Pd NPs were. Among the silica-based systems, those prepared under acidic conditions are the most active, exhibiting higher TOF in comparison to those of isolated Pd NPs. The denser and bulkier structure generated under basic conditions might have afforded less active systems as shown by some clues. First, the ionic liquids content, which seems to be important in order to guarantee stability for the nanoparticles, was lower for these systems. Besides, according to porosimetric measurements, the pore diameter was much smaller for the SiO_2/ILs/PdNPs/NH_4OH system. Palladium encapsulated particles, in spite of a slightly higher content in comparison to that afforded with an acid catalyst (Table 3), might be not accessible in the supported systems prepared under basic conditions. The hydrogenation of simple arenes and alkenes by SiO_2/ILs/Pd NPs/HF depends on steric hindrance at the C=C double bond and follows the same trend as observed with classical palladium complexes in homogeneous conditions, that is, the reactivity follows the order: terminal-internal.

Conclusions

Palladium nanoparticles dispersed in ionic liquids and functionalized ionic liquids (SiO_2/ILs/Pd NPs) can be easily immobilized within a silica network when prepared by the sol-gel method (acid or base catalysis). The palladium content in the resulting xerogels was shown to be independent of the preparative route, but acidic conditions afforded higher encapsulated ionic liquid content and xerogels with larger pore diameter, which in turn might have guaranteed higher catalyst activity in the hydrogenation of arenes and alkenes. The use of ionic liquids for the preparation of both nanoparticles and silica affords encapsulated SiO_2/ILs/Pd NPs materials with different morphology, texture, and catalytic activity. This combination exhibits an excellent synergistic effect that enhances the stability and activity of the Pd NPs in hydrogenation catalysts. All the supported systems were more active than that constituted of isolated Pd NPs for the hydrogenation of arenes and alkenes. In particular, the silica-based systems prepared under acidic conditions were shown to be the most active, exhibiting higher TOF. The denser and bulkier silica structure generated under basic conditions (less active catalytic system) incorporated less ionic liquids. A high level of ionic liquids incorporation seems to be important in order to guarantee stability for the palladium nanoparticles.

Acknowledgements

Thanks are due to the following Brazilian Agencies: CNPq, CAPES, FAPERGS for fellowships and partial financial support.

References

1. Mehnert CP. Supported ionic liquid catalysis (2004) Chem Eur J 11: 50-56. https://doi.org/10.1002/chem.200400683
2. Faria VW, Scheeren CW, Rosa GR, Kurz MHS, Gonçalves FF, et al. Palladium nanoparticles supported in a polymeric membrane: an efficient phosphine-free "green" catalyst for suzuki-miyaura reactions in water (2014) RSC Advances: an intern j to further the chem sci 4: 13446-13452. https://doi.org/10.1039/c4ra01104j
3. Scheeren CW, Fischer DK and Fraga KR. Chitosan microspheres from shrimp waste supporting pd nanoparticles in ionic liquids: an efficient and eco-friendly catalyst for hydrogenation reactions (2020) J of Nanoscience and Nanotechnology 20: 1296-1302. https://doi.org/10.1166/jnn.2020.16964
4. Riisager A, Fehrmann R, Haumann M and Wasserscheid P. Supported ionic liquids: versatile reaction and separation media (2006) Top Catal 40: 91.
5. Sharma AS, Kaur H and Shah D. Selective oxidation of alcohols by supported gold nanoparticles: recent advances (2016) RSC Adv 6: 28688-28727. https://doi.org/10.1039/c5ra25646a
6. Rioux RM, Song H, Grass M, Habas S, Niesz K, et al. Monodisperse platinum nanoparticles of well-defined shape: synthesis, characterization, catalytic properties and future prospects (2006) Top catal 39: 167-174. https://doi.org/10.1007/s11244-006-0053-2
7. Verga LG, Russell A and Skylaris CK. Ethanol, O, and co adsorption on pt nanoparticles: effects of nanoparticle size and graphene support (2018) Phys Chem Chem Phys 20**:** 25918-25930. https://doi.org/10.1039/c8cp04798g

8. Riisager A, Fehrmann R, Haumann M and Wasserscheid P. Supported ionic liquid phase (silp) catalysis: an innovative concept for homogeneous catalysis in continuous fixed-bed reactors (2006) Eur J Inorg Chem 695. https://doi.org/10.1002/ejic.200500872
9. Schmies H, Bergmann A, Hornberger E, Drnec J, Wang G, et al. Anisotropy of pt nanoparticles on carbon- and oxide-support and their structural response to electrochemical oxidation probed by in situ techniques (2020) Phys Chem Chem Phys 22: 22260-22270. https://doi.org/10.1039/d0cp03233f
10. Maity N, Sahoo A, Boddhula R, Chatterjee S, Panda BB, et al. Fly ash supported pd–ag bimetallic nanoparticles exhibiting a synergistic catalytic effect for the reduction of nitrophenol (2020) Dalton Trans 49: 11019-11026. https://doi.org/10.1039/d0cp03233f
11. Mehnert CP, Cook RA, Dispenziere NC and Afeworki M. Supported Ionic Liquid Catalysis -A New Concept for Homogeneous Hydroformylation Catalysis (2002) J Am Chem Soc 124: 12932-12933. https://doi.org/10.1021/ja0279242
12. Brett GL, Miedziak PJ and Dimitratos N. (2012) Catal Sci Technol 2: 97-104.
13. Webb PB, Kunene TE and Cole-Hamilton DJ. Continuous flow homogeneous hydroformylation of alkenes using supercritical fluids (2005) Green Chem 7: 373. https://doi.org/10.1039/B416713A
14. Miyazaki A, Matsuda K, Papa F, Scurtu M, Negrila C, et al. Impact of particle size and metal–support interaction on denitration behavior of well-defined Pt–Cu nanoparticles (2015) Catal Sci Technol 5: 492-503. https://doi.org/10.1039/C4CY00929K
15. deCastro C, Sauvage E, Valkenberg Mh and Holderich WF. Immobilised Ionic Liquids as Lewis Acid Catalysts for the Alkylation of Aromatic Compounds with Dodecene (2000) J Catal 196: 86-94. https://doi.org/10.1006/jcat.2000.3004
16. Mehnert CP, Mozeleski EJ and Cook RA. Supported ionic liquid catalysis investigated for hydrogenation reactions (2002) Chem Commun 3010-3011. DOI https://doi.org/10.1039/B210214E
17. Hagiwara H, Sugawara Y, Isobe K, Hoshi T and Suzuki T. Immobilization of Pd(OAc)(2) in ionic liquid on silica: application to sustainable Mizoroki-Heck reaction (2004) Org Lett 6: 2325-2328. https://doi.org/10.1021/ol049343i
18. Breitenlechner S, Fleck M, Muller TE and Suppan A. Solid catalysts on the basis of supported ionic liquids and their use in hydroamination reactions (2004) J Mol Catal A Chem 214: 175-179. https://doi.org/10.1016/j.molcata.2003.12.032
19. Dupont J and Suarez PAZ. Physico-chemical processes in imidazolium ionic liquids (2006) Phys Chem Chem Phys 8: 2441. https://doi.org/10.1039/b602046a
20. Consorti CS, Suarez PAZ, de Souza RF, Burrow RA, Farrar DH, et al. CCDC 268404: Experimental Crystal Structure Determination (2005) J Phys Chem B 109: 4341.
21. Dupont J. On the solid, liquid and solution structural organization of imidazolium ionic liquids (2004) J Braz Chem Soc 15: 341. https://doi.org/10.1590/S0103-50532004000300002
22. Antonietti M, Kuang DB, Smarsly B and Yong Z. Ionic liquids for the convenient synthesis of functional nanoparticles and other inorganic nanostructures (2004) Angew Chem Int Ed 43: 4988. https://doi.org/10.1002/anie.200460091
23. Zhou Y and Antonietti M. Synthesis of very small tio_2 nanocrystals in a room-temperature ionic liquid and their self-assembly toward mesoporous spherical aggregates (2003) J Am Chem Soc 125: 14960-14961. https://doi.org/10.1021/ja0380998
24. Zhou Y, Schattka JH and Antonietti M. Room-temperature ionic liquids as template to monolithic mesoporous silica with wormlike pores via a sol-gel nanocasting technique (2004) Nano Lett 4: 477-481. https://doi.org/10.1021/nl025861f
25. Jin R , Zeng C, Zhou M and Chen Y. Atomically precise colloidal metal nanoclusters and nanoparticles: fundamentals and opportunities (2016) Chem Rev 116: 10346-413. https://doi.org/10.1021/acs.chemrev.5b00703
26. Dai S, Ju YH, Gao HJ, Lin JS, Pennycook SJ, et al. Preparation of silica aerogel using ionic liquids as solvents (2000) Chem Commun 243-244. https://doi.org/10.1039/a907147d
27. Scheeren CW, Machado G, Teixeira SR, Morais J, Domingos Jb, et al. Synthesis and characterization of Pt0 nanoparticles in imidazolium ionic liquids (2006) J Phys Chem B 110: 13011-13020. https://doi.org/10.1021/jp0623037
28. Silveira ET, Umpierre AP, Rossi LM, Machado G, Morais J, et al. The partial hydrogenation of benzene to cyclohexene by nanoscale ruthenium catalysts in imidazolium ionic liquids (2004) Chem Eur J 10: 3734-3740. https://doi.org/10.1002/chem.200305765
29. Dupont J, Fonseca Gs, Umpierre AP, Fichtner PFP and Teixeira SR. Transition-metal nanoparticles in imidazolium ionic liquids: recyclable catalysts for biphasic hydrogenation reactions (2002) J Am Chem Soc 124: 4228-4229. https://doi.org/10.1021/ja025818u
30. Dupont J and Migowski P. Catalytic applications of metal nanoparticles in imidazolium ionic liquids (2007) Chem Eur J 13: 32-39. https://doi.org/10.1002/chem.200601438
31. Mu XD, Evans DG and Kou YA. A general method for preparation of PVP-stabilized noble metal nanoparticles in room temperature ionic liquids (2004) Catal Lett 97: 151-154. https://doi.org/10.1023/b:catl.0000038577.18441.bf
32. Mu XD, Meng JQ, Li ZC and Kou Y. Rhodium nanoparticles stabilized by ionic copolymers in ionic liquids: long lifetime nanocluster catalysts for benzene hydrogenation (2005) J Am Chem Soc 127: 9694-9695. https://doi.org/10.1021/ja051803v
33. Miao SD, Liu ZM, Han BX, Huang J, Sun ZY, et al. Ru nanoparticles immobilized on montmorillonite by ionic liquids: a highly efficient heterogeneous catalyst for the hydrogenation of benzene (2006) Chem Int Ed 45: 266-269. https://doi.org/10.1002/anie.200502632
34. Huang J, Jiang T, Han B and Wu W. A novel method to immobilize ru nanoparticles on sba-15 firmly by ionic liquid and hydrogenation of arene (2005) Catal letters 103: 59-62. https://doi.org/10.1007/s10562-005-6503-9
35. Mevellec V, Nowicki A, Roucoux A, Dujardin C, Granger P, et al. A simple and reproducible method for the synthesis of silica-supported rhodium nanoparticles and their investigation in the hydrogenation of aromatic compounds (2006) New J Chem 30: 1214-1219. https://doi.org/10.1039/b605893k
36. Li S, Liu M, Zhang A and Guo X. Spherical mesoporous silica templated with ionic liquid and cetyltrimethylammonium bromide and its conversion to hollow spheres (2010) materials letters 64: 599-601. https://doi.org/10.1016/j.matlet.2009.12.013
37. Moseley K and Maitlis PMJ. Bis- and tris-(dibenzylideneacetone)platinum and the stabilization of zerovalent complexes by an unsaturated ketone (1971) Chem Soc Chem Commun 982-983. https://doi.org/10.1039/c29710000982
38. Cassol CC, Ebeling G, Ferrera B and Dupont J. A simple and practical method for the preparation and purity determination of halide-free imidazolium ionic liquids (2006) Adv Synth Catal 348: 243. https://doi.org/10.1002/adsc.200505295
39. Carvajal JR. Introduction to the program fullprof. laboratoire leon brillon (cea-cnrs), saclay france (2004)
40. Schubert U and Husing N. Inorganic Materials: A Chemical Approach 1st edn Wiley Weinheim **2000**.
41. Bernardi F, Alves MCM, Traverse A, Silve DO, Scheeren CW, et al. (2009) J Phys Chem 113: 3909.
42. Vansant EF, Van Der Voort P and Vrancken KC. Characterization and Chemical Modification of the Silica Surface.